

EFTEM-HRTEM characterization of Er-doped silicon nanocrystal-based oxides/nitrides for MOS light emitting devices

Alicia Ruiz Caridad

*Supervisors: Francesca Peiro Martínez and Sònia Estradé Albiol
Departament d'Electrònica, Universitat de Barcelona,*

Abstract: Er-doped silicon nanocrystal-based oxides/nitrides have been investigated. These layers are grown between a polycrystalline silicon electrode and a monocrystalline silicon substrate to allow electrical injection. Energy Filtered (EF-) and High Resolution (HR-) TEM characterization has been performed to provide microscopic insight onto the macroscopic optoelectronic properties of the samples. Evident Er-clustering has been observed in silicon dioxides but not in silicon nitrides, suggesting a better Er solubility and local environment when nitrogen is incorporated. Silicon nanocrystals have been observed in silicon-rich nitride layers, as expected, but also in a region close to the silicon dioxide-polysilicon interface in a layer with no nitrogen or Si excesses. This unexpected Si clusterization has been attributed to Si diffusion from the polycrystalline silicon electrode into the silicon dioxide as a consequence of the annealing treatment. The structural characterization carried out by HRTEM and EFTEM has been correlated with the optoelectronic properties of the devices.

I. INTRODUCTION

Er-doped materials have attracted strong interest during the last decades as an optical material enabling advanced telecommunications applications. A fast development in long-haul optical data transmission was possible with the implementation of Erbium Doped Fibre Amplifiers (EDFA). Similarly, a fast development in on-chip data transfer rates is expected from integrated optic solutions. Such approach would provide an effective alternative for the interconnect microelectronics bottleneck [1]. Therefore, many efforts are being devoted to develop an electrically driven light emitting source emitting at 1.54 μm compatible with the mainstream Complementary Metal Oxide Semiconductor (CMOS) technology. Among others, Er-doped oxides are good candidates for developing Er-doped light emitting devices due to the good local environment provided for the Er ions, as well as their outstanding electrical and thermal stabilities [2]. Nevertheless, the large band gap of silicon dioxide makes the Er excitation via current injection difficult. Therefore, it is interesting to study other CMOS compatible matrices with lower band gaps and suitable to accommodate Er ions. In this sense, silicon nitride provides ideal characteristics, as it is a good host for Er ions, it is electrically and thermally stable, and has a lower band gap, that would allow for larger current injection compared to silicon dioxide. Moreover, current injection can be further boosted by embedding silicon nanocrystals (Si-NCs) in the matrix [3]. Surprisingly, in spite of the great amount of works devoted to the study of these materials, not many of them focus on the correlation between microstructure and optical efficiency.

This work will focus on the study of four different systems, all of them Er-doped layers sandwiched between a monocrystalline Si substrate and a polycrystalline silicon electrode, the layers consisting on: silicon dioxide (SiO_2); silicon nitride (Si_3N_4); silicon-rich nitride (SiN_x); and silicon oxynitride (SiON) which provides a mid-point between SiO_2 and Si_3N_4 .

In order to improve the functional properties of a given system, it is essential to determine its local structure and composition. To improve the optical efficiency it is essential to know the material distribution and structure. Transmission Electron Microscopy (TEM) can provide a complete characterization of nanoscale materials and devices. TEM is based on the interaction between a fast electron and a solid state sample. When the incoming electron interacts with the periodic potential of a crystal, its wave function can suffer changes both in amplitude and phase. In most situations both types of contrast (amplitude contrast and phase contrast) contribute to an image, though one of them will tend to dominate

High Resolution TEM (HRTEM) is related to phase contrast. Interaction between electron beams diffracted by different families of planes amongst themselves and with the undiffracted beam gives rise to a periodic contrast, parallel to a given family of planes and with a periodicity related to its spacing [4][8]. Energy Filtered TEM (EFTEM) is based on a very different physical interaction taking place in the microscope. The incoming fast electron can transfer a given amount of energy to electrons in the sample; this energy loss can be measured with a magnetic prism, which is how Electron Energy Loss Spectroscopy (EELS) is performed. An EELS spectrum is, thus, a plot showing how many electrons

have lost which amount of energy. Now, if the energy filter is used as a band-pass filter, an EFTEM image will be obtained, from the contribution of electrons having lost energy in a given energy loss interval only [9].

II. EXPERIMENTAL DETAILS

A. Sample growth

Samples were provided by the CIMAP laboratory in France. The active layers were grown by magnetron sputtering on a p-type silicon substrate at 500°C. Different approaches were used in order to obtain different stoichiometries in the samples. The SiO₂:Er sample was obtained from direct evaporation of a SiO₂ target and an Er₂O₃ target. The SiON:Er samples were grown using three cathodes, one for Si₃N₄, one for SiO₂ and one for Er₂O₃. A bias was applied to each cathode to enhance the deposition rate flow into the substrate. Finally the SiN_x samples were grown with a two cathode approach, cathodes corresponding to SiO₂ and Er₂O₃, while nitrogen was added by introducing a N flow in to the chamber. The silicon excess of the SiN_x samples was obtained by varying the nitrogen flow and keeping the other parameters constant. A silicon excess value of 30% was measured. A nominal thickness of 50 nm was targeted for all samples. To perform the electrical pumping of the samples and the light collection, a polycrystalline silicon electrode (polysilicon) of 200nm was deposited on top of the active layer by low pressure chemical vapour deposition (LPCVD). Subsequently, an annealing treatment at 950°C for 30 minutes in a nitrogen atmosphere was carried out. The polysilicon layer is devised to act as both an electrode for current injection and as a semitransparent window to efficiently extract the generated electroluminescence (EL). In order to certify the inclusion of Er ions in the matrix, secondary ion mass spectrometry (SIMS) was performed in all samples, yielding an Er concentration of $1 \times 10^{20} \text{ cm}^{-3}$ in all samples. Similarly, X-Ray photoelectron spectroscopy (XPS) was carried out to determine the sample composition in each sample. Further details can be found in [5].

B. EFTEM and HRTEM

For EFTEM and HRTEM characterization a JEOL 2010F microscope coupled to a post-column Gatan Imaging Filter (GIF), in the CCiTUB facilities, was used. Samples for TEM observation were obtained in cross-section geometry by conventional preparation methods. Samples were mechanically polished to a 60 μm thickness. Further dimple polishing was performed down to 20 μm. Finally, electrotransparency was achieved by low angle Ar⁺ ion

milling (5KeV, 7° and 4°) using a Gatan PIPS instrument. Prior to TEM observation samples were cleaned using a 25% O and 75% Ar plasma.

C. Opto-electronic Characterization

The electrical characteristics of the samples were analyzed using a semiconductor device analyzer (B1500A) coupled to a probe station (Cascade Microtech Submmitt 1100). The electroluminescence (EL) spectra were collected with a photomultiplier tube (PMT) coupled to a monochromator (Acton 20300i) under forward bias condition.

III. RESULTS AND DISCUSSION

Fig.1 (a) shows a typical EL spectrum, with a maximum intensity around of 1.54 μm. It is worth noticing that the spectrum did not change with current injection, or in the different devices. The observed emission is a consequence of the discrete transition of Er³⁺ ions from the first excited state to the ground level. Electrons are injected from the polysilicon electrode into the active layer and excite Er³⁺ ions by inelastic scattering.

Fig.1 (b) displays a comparison of the emitted EL (in arbitrary units) as a function of the injected current (in A) for all studied devices. All samples show a linear increase in EL with injected current. We can compare the quantum efficiency of the different devices by direct inspection of Fig.1 (b). Quantum efficiency stands for the ratio between generated photons and injected electrons. Therefore, data in Fig.1 (b) allow us to conclude that: (i) the SiO₂:Er sample is the most efficient one, as it requires the lowest injected current for EL; (ii) the incorporation of nitrogen in the matrix gradually reduces the efficiency of the injected electrons, as demonstrated by comparing SiO₂:Er (no nitrogen), SiON:Er (low nitrogen incorporation) and Si₃N₄:Er (higher nitrogen incorporation); and (iii) The incorporation of Si excess improves the efficiency (compare the Si₃N₄:Er curve with the SiN_x:Er one).

Hence, different optoelectronic properties are found in the different systems. In order to gain further insight on the structural properties of these samples, TEM characterization was performed. This characterization is meant to assess the quality of the systems, for instance, the abruptness of the interfaces between the active layer and the electrode (polysilicon, in this case). Also, the presence of Si-NCs was inspected, as well as the possible Er clusterization.

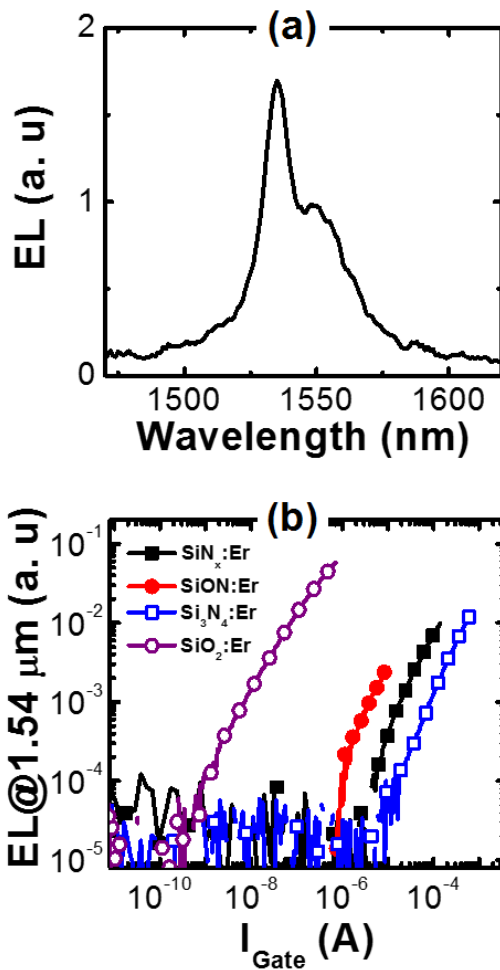


FIG. 1: (a) EL spectrum of $\text{SiO}_2:\text{Er}$ sample taken at 10^{-8} A. (b) EL at $1.54 \mu\text{m}$ as a function of injected current for the $\text{SiN}_x:\text{Er}$ sample (black squares), the $\text{SiON}:\text{Er}$ (red dots), the $\text{Si}_3\text{N}_4:\text{Er}$ (blue empty squares) and the $\text{SiO}_2:\text{Er}$ (purple empty dots).

Fig. 2 (a) shows a general view of TEM image of the $\text{SiO}_2:\text{Er}$ system. Three different layers can be observed: the Si substrate (top layer), the $\text{SiO}_2:\text{Er}$ (middle layer) and the polysilicon electrode (bottom). A mean thickness of 85 nm was measured for the $\text{SiO}_2:\text{Er}$. Well defined interfaces are observed, with no presence of unwanted native oxide between the Si substrate and the $\text{SiO}_2:\text{Er}$ layer. Abrupt interfaces are important to validate the suitability of the fabrication process to develop electroluminescent devices.

In order to determine the presence of Si nanocrystals (NCs) in the $\text{SiO}_2:\text{Er}$ layer, an EFTEM image was taken. For that, the crystalline Si plasmon peak (15 eV) was filtered, obtaining bright zones wherever there is crystalline Si (Fig. 2 (b)). Notice that the $\text{SiO}_2:\text{Er}$ layer presents Si-NCs randomly distributed within a depth of approximately 39 nm from the polysilicon interface (bottom part of Fig. 2 (b)). Despite silicon excess was not expected in the $\text{SiO}_2:\text{Er}$ layer, its presence could be explained by an eventual silicon migration from the polysilicon towards the $\text{SiO}_2:\text{Er}$ layer as a consequence of

the high annealing temperature performed to the sample. This fact explains why silicon nanocrystals are found in the 39 nm closest to the polysilicon layer only and not everywhere in the sample. In order to further corroborate this hypothesis, the same procedure was performed at the other interface, i.e. at the Si substrate- $\text{SiO}_2:\text{Er}$ interface (Fig.3). In that case, dark spots are also observed in the HRTEM image. However, they do not correspond to Si-NCs, as the EFTEM image obtained by filtering the Si plasmon peak did not show any bright spots in the $\text{SiO}_2:\text{Er}$ layer. To further discard the presence of Si-NCs or other oxydized phases of SiO_2 , an additional EFTEM image was taken by filtering the SiO_2 plasmon peak (23 eV) instead of that of silicon (Fig. 3 (c)). In that case, dark spots are still observed in the image. Thus, we can unambiguously confirm that the dark spots should correspond to Er clustering.

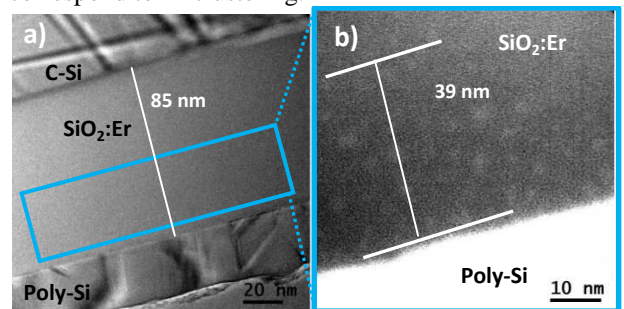


FIG. 2: $\text{SiO}_2:\text{Er}$ system (a) general TEM image and further magnified EFTEM image (b) showing Si-NCs) located within 39 nm of the polysilicon layer.

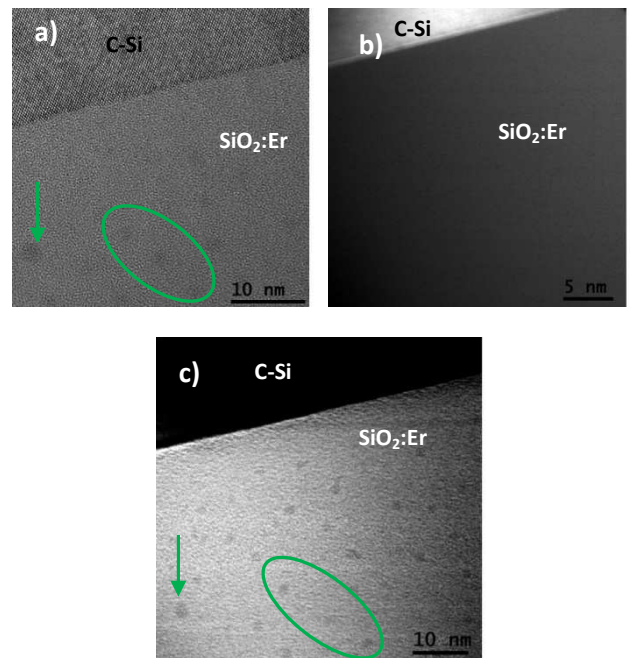


FIG. 3: $\text{SiO}_2:\text{Er}$ system near at the substrate / active layer interface (a) HRTEM image, (b) crystalline Si plasmon energy filtered image and (c) SiO_2 plasmon energy filtered image of the same region. The same features can be observed in (a) and (c) as highlighted by the arrow and the circle distributed.

A similar analysis was performed for the $\text{Si}_3\text{N}_4:\text{Er}$ system (Fig. 4 and 5). Layer thickness was determined to be around 51 nm, in good agreement with the expected nominal value (i.e. 50 nm). In this case, however, nor Si-NCs neither Er clustering was found when filtering by both the silicon and the SiO_2 plasmon peak. Lattice fringes corresponding to crystalline silicon are observed in the EFTEM image filtered by the silicon plasmon peak (Fig. 5 (b)).

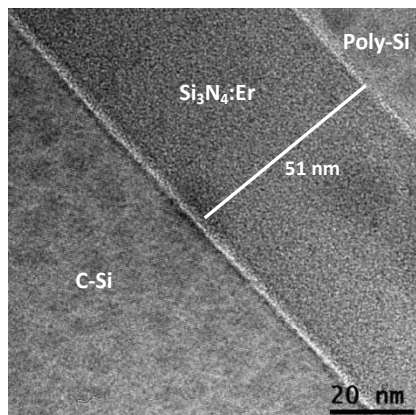


FIG. 4: General TEM image of the $\text{Si}_3\text{N}_4:\text{Er}$ system.

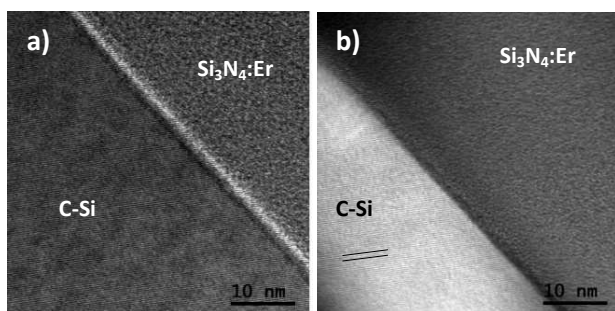


FIG. 5: $\text{Si}_3\text{N}_4:\text{Er}$ system near the substrate / active layer interface (a) HRTEM image and (b) EFTEM image, filtered at the crystalline silicon plasmon energy, of the same region

The $\text{SiON}:\text{Er}$ system was also inspected using TEM and EFTEM (Fig. 6). A layer thickness of 52 nm was obtained, similar to the one obtained for $\text{Si}_3\text{N}_4:\text{Er}$. No Si-NCs or Er clusters were found. Thus the $\text{SiON}:\text{Er}$ and $\text{Si}_3\text{N}_4:\text{Er}$ systems present very similar morphological properties.

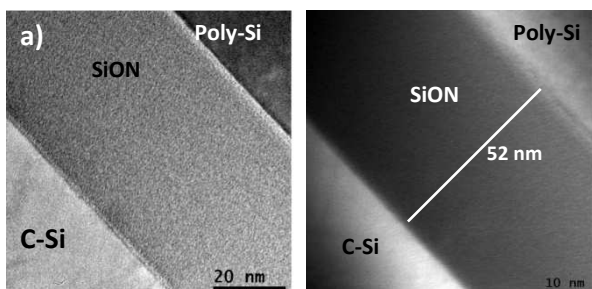


FIG. 6: General TEM (a) and EFTEM (filtered at crystalline Si plasmon energy) (b) images of the $\text{SiON}:\text{Er}$ system. No Si-NCs or Er clusters are observed

Finally, the $\text{SiN}_x:\text{Er}$ system was also analyzed (Fig.7). This is an interesting case of study, as this is the only sample in which Si-NCs were intentionally incorporated. Surprisingly, an unexpectedly thin $\text{SiN}_x:\text{Er}$ layer of 8.4 nm was observed, despite the fact that the nominal deposition thickness was set to 50 nm. The origin of this discrepancy is not well understood yet and thus deserves a thorough investigation that lies beyond the scope of the present work.

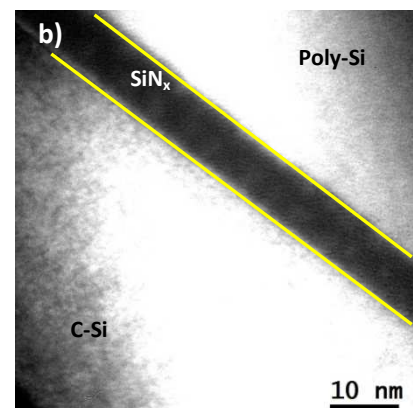
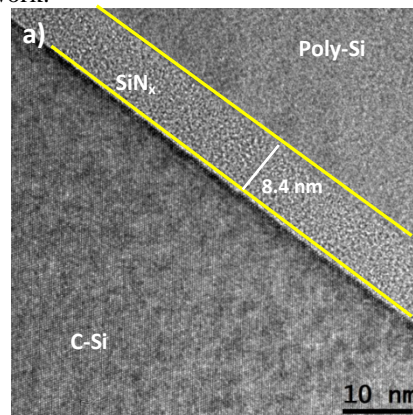


FIG. 7: (a) HRTEM image and (b) EFTEM image, filtered at the crystalline silicon plasmon energy, of the same region, containing the $\text{SiN}_x:\text{Er}$ layer

As for the Si incorporation, it is clear that Si-NCs are present in the layer, as observed in Fig. 7 (b) EFTEM image filtered by the Si plasmon peak shows bright zones within the active layer which correspond to the Si-NCs.

Thus, only the $\text{SiO}_2:\text{Er}$ presented evident Er clustering. At this point, it is worth highlighting that the fact that no Er clustering was observed by TEM in the other active layers ($\text{Si}_3\text{N}_4:\text{Er}$, $\text{SiON}:\text{Er}$ and $\text{SiN}_x:\text{Er}$) does not completely rule out small Er agglomeration of few atoms, below the TEM resolution limit. However, even if that was the case, we can safely conclude that the $\text{SiO}_2:\text{Er}$ system has the largest Er clustering among the studied samples. The reason for this could lie in a different solubility of Er ions in SiO_2 compared to the other matrices. Lower Er solubility in SiO_2 is expected. Another interesting conclusion that could be directly derived from this study is that nitrogen incorporation seems to consistently reduce the Er clustering in the layer, as nitrogen-based samples did not show evident Er clusterization. In

addition, notice that Er clustering shows a direct correlation with the optoelectronic properties of samples, as it strongly diminishes the luminescence [6]. Er clustering provides an undesired local environment for Er^{3+} ions, making them optically inactive (i.e.: non light-emitting). In spite of this fact, the $\text{SiO}_2\text{:Er}$ system is still the most efficient device among the studied samples (see Fig.1 (b)). This means that room for improvement is expected at least for the $\text{SiO}_2\text{:Er}$ device in terms of quantum efficiency if an optimized $\text{SiO}_2\text{:Er}$ system free of Er-clustering is fabricated.

As for the Si-NCs, they were successfully incorporated in the silicon nitride layer. Nevertheless, an unexpectedly low layer thickness was observed in this sample. Also, Si-NCs were unexpectedly observed in the $\text{SiO}_2\text{:Er}$ layer. In this case, however, they were not uniformly distributed, as in the $\text{SiN}_x\text{:Er}$ layer. They were only visible near the active layer / electrode interface (see Fig.2). The presence of these NCs can be explained by the diffusion of Si atoms from the polysilicon electrode to the $\text{SiO}_2\text{:Er}$ layer as a consequence of the annealing treatment performed on the sample. As a matter of fact, this Si diffusion was not observed in the other silicon nitride-based samples, suggesting that nitrogen incorporation effectively blocks the Si diffusion from the polysilicon electrode. Two possible alternatives could be considered to avoid Si diffusion into the $\text{SiO}_2\text{:Er}$ layer: (i) an effective reduction of the annealing treatment parameters (either annealing time or temperature), and (ii) the inclusion of a silicon nitride diffusion barrier between the SiO_2 and the polysilicon electrode. Finally, the observation of Si-NCs in the $\text{SiN}_x\text{:Er}$ layer is in good agreement with the optoelectronic properties shown in Fig.1 (b). In particular, the improvement of quantum efficiency of the $\text{SiN}_x\text{:Er}$ system compared to $\text{Si}_3\text{N}_4\text{:Er}$ system could be unambiguously correlated with the presence of Si-NCs. In fact, previous works on this subject have already demonstrated an efficient energy transfer mechanism from

Si-NCs to Er ions that enhances the luminescent properties [7].

IV. CONCLUSIONS

- Er-doped silicon nanocrystal-based oxide/nitride light emitting devices were characterized first by studying their electrical-optical response and then by HRTEM and EFTEM.
- Four different systems with different active layer stoichiometry values have been studied: silicon dioxide (SiO_2), silicon nitride (Si_3N_4) silicon-rich nitride (SiN_x) and silicon oxynitride (SiON), all of them with the same Er concentration.
- Unexpected silicon nanocrystals and Er clustering were observed in the $\text{SiO}_2\text{:Er}$ layer, the first attributed to a Si diffusion from the polysilicon electrode during thermal annealing, and the second to a low Er solubility in SiO_2 .
- No Er clustering was observed when incorporating nitrogen to the matrix, suggesting better Er solubility in nitrogen-based materials.
- Silicon nanocrystals were otherwise, only observed in the silicon-rich nitride sample, as expected. Better quantum efficiency was obtained when embedding Si-NCs.

Acknowledgments

I would like to specially thank my advisors Francesca Peiró and Sònia Estradé for their help and support as to LENS group in Universitat de Barcelona for their patience and training. We acknowledge CIMAP at Caen laboratory for sample fabrication, electro-photonics group in Universitat de Barcelona and to CCIT-UB facilities.

- | | |
|--|---|
| <p>[1] B. Jalali et al, «Silicon photonics,» <i>J. Lightwave Technol.</i>, pp.4600-4615, 2006.</p> <p>[2] J. M. Ramírez et al, «Optimizing Er-doped Layer Stacks for Integrated Light Emitting Devices,» <i>ECS Trans.</i>, pp. 81-84, 2013.</p> <p>[3] S.Cueff et al, «Electroluminescence efficiencies of erbium in silicon-based hosts,» <i>Appl.Phys. Lett.</i>, pp. 103, 2013.</p> <p>[4] D. B. Williams and C.B. Carter. <i>Transmission Electron Microscopy</i>. Second edition.</p> <p>[5] S. Cueff et al et al, «Silicon-rich oxynitride hosts for 1.5 μm Er^{3+} emission fabricated by reactive and standard RF magnetron sputtering,» <i>Materials Science and Engineering: B.</i>, pp. 725-728, 2012.</p> | <p>[6] N. Prtljaga et al, «Limit to the erbium ions emission in silicon-rich oxide films by erbium ionclustering,» <i>Optical Materials Express</i>, pp. 1278-1285, 2012.</p> <p>[7] S. Yerci et al, «Electroluminescence from Er-doped Si-rich silicon nitride light emitting devices,» <i>Appl. Phys. Lett.</i>, pp. 081109(3), 2010.</p> <p>[8] L. López-Conesa. <i>EFTEM-HRTEM characterization of Si nanocrystals embedded in a multilayer matrix for tandem solar cell applications</i>. Universitat de Barcelona. Tesis de Master (2011)</p> <p>[9] R. F. Egerton. <i>Electron Energy-Loss Spectroscopy in the Electron Microscope</i>. Third edition.</p> |
|--|---|